

Energy Relaxation and Non-linear Transport in InAs Nanowires

R Hathwar, M Saraniti and S M Goodnick

Center for Computational Nanoscience, Arizona State University, USA

E-mail: rhathwar@asu.edu

Abstract. Using a full band Monte Carlo simulation the electron energy relaxation times of InAs nanowires along the [100] direction are shown to be greater than the energy relaxation time of bulk InAs. The full band structure and scattering rates of the nanowires are calculated using the $sp^3d^5s^*$ tight binding method and Fermi's Golden rule respectively. At moderately high electric fields, a runaway effect is also observed in the nanowires and is attributed to the 1D nature of the scattering rates.

1. Introduction

In recent years nanowires have become important as both a novel material and as a channel for transistors. Various companies are researching the usefulness of nanowire field effect transistors (FETs) as a possibility for devices with very small gate lengths. It is therefore very important to understand the material properties of nanowires and create models that can simulate transport in nanowires. In particular, the energy relaxation rates are of interest in terms of advanced concept photovoltaic devices based on hot carrier extraction [1]. Materials with a larger relaxation time lead to higher efficiency in solar cells based on hot carrier extraction. Also non-equilibrium behavior of nanowires is of high importance in simulating FETs and is therefore important to correctly model the behavior of nanowires in non-equilibrium conditions.

In section 2 the method used to simulate nanowires under photoexcitation as well as under high fields is discussed. In section 3 the results are discussed.

2. Simulation Method

The band structure of InAs nanowires are calculated using the $sp^3d^5s^*$ empirical tight binding method including spin. This method has accurately modelled the band gap and effective masses of nanowires and is used widely in the literature [2]. In this work a k-space Monte Carlo simulation is performed to simulate the high field and non-equilibrium properties of InAs nanowires. The 1D scattering rates needed for such a simulation are calculated using the Fermi's golden rule. Polar optical phonon scattering rates and deformation potential scattering rates are included in the simulation. The scattering rate for acoustic phonons using the equipartition approximation is [3],

$$W_{ac,\mu,\nu}(k,k') = \frac{E_{ac}^2 kT}{4\pi\rho v_s^2 \hbar} I_{\mu,\nu}(\mathbf{q}) \text{DOS}(k') \quad (1)$$



and the scattering rate for optical phonons assuming dispersionless phonons is

$$W_{op,\mu,\nu}(k,k') = \frac{E_{op}^2}{4\pi\rho\omega_{op}} \left(N_{q,op} + \frac{1}{2} \pm \frac{1}{2} \right) I_{\mu,\nu}(\mathbf{q}) \text{DOS}(k') \quad (2)$$

where

$$I_{\mu,\nu}(\mathbf{q}) = \sum_m \sum_{m'} c_{\nu,m}^*(k') c_{\mu,m}(k) c_{\mu,m'}^*(k) c_{\nu,m'}(k') q_c \frac{J_1(q_c a_{diff})}{a_{diff}} e^{iq[\tau_{m,x} - \tau_{m',x}]} \quad (3)$$

where $a_{diff} = \sqrt{(\tau_{m,y} - \tau_{m',y})^2 + (\tau_{m,z} - \tau_{m',z})^2}$ and the sum is over all orbitals in the supercell. $q_c \approx 1.9\pi/a$ is used as an effective cut-off radius to emulate the projection of the BZ of bulk material onto the confinement plane [4]. E_{ac} and E_{op} are the deformation potential constants for the acoustic and optical modes respectively, v_s is the sound velocity in InAs, μ and ν are the initial and final band indices and ω_{op} is the wavenumber for the optical phonons. The scattering rate for the polar optical phonons is given by [5]

$$W_{pop,\mu,\nu}(k,k') = \frac{\omega_0 e^2}{8\pi} \left[\frac{1}{\epsilon_\infty} - \frac{1}{\epsilon_0} \right] \left(N_{|q|,op} + \frac{1}{2} \pm \frac{1}{2} \right) I_{pop,\mu,\nu}(\mathbf{q}) \quad (4)$$

where

$$I_{pop,\mu,\nu}(\mathbf{q}) = \sum_m C_{\mu,m}(k) C_{\nu,m}^*(k') \sum_{m'} C_{\mu,m'}^*(k) C_{\nu,m'}(k') \int_0^{q_c} \frac{J_0(q_t a_{diff})}{q^2 + q_t^2} e^{iq[\tau_{m,x} - \tau_{m',x}]} q_t dq_t \quad (5)$$

where q_t is the phonon vector along the confinement plane. The integral in equation (5) can be pre-calculated for a fixed number of q_t values. This speeds up the computational time during the scattering rate calculation. It is important to note that when the scattering rates for bulk InAs and InAs nanowires are compared, they show an agreement at high energies for the same deformation potential and tight binding parameters as shown in figure (2). This agreement provides credibility to the tight binding method when scaling from bulk to nano-systems.

The agreement in the scattering rates result in an agreement of the high field velocity curves between bulk and nanowire InAs as shown in figure (3). To simulate hot carrier relaxation during photoexcitation the electrons are initialized with a mean energy corresponding to the excitation energy of the photons. A Gaussian half-width of 100meV is used. The momentum of the carrier is uniformly distributed across the Brillouin Zone. The Monte Carlo simulation is then ran until the average energy of the carriers remains a constant with respect to time. To calculate the energy relaxation time no electric field is applied to the carriers, and the carrier relax according to the scattering rates of the system.

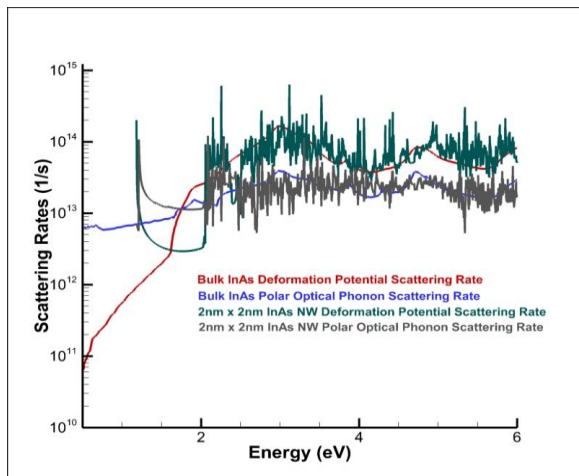


Figure 1. Comparison of the polar optical and deformation potential scattering rates between a 2nmx2nm InAs NW along [100] and bulk InAs using the same parameters.

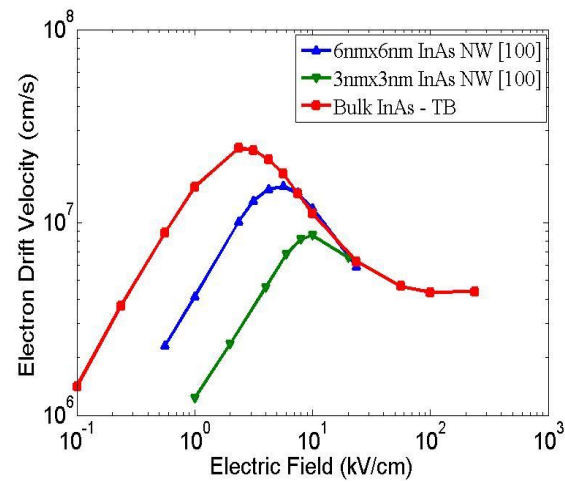


Figure 2. Comparison of drift velocity field curves between Bulk InAs and 3nmx3nm and 6nmx6nm InAs nanowires along [100].

3. Results

The electrons are initialized with a mean energy corresponding to the excitation energy shown in figure (3). After a few picoseconds the initial distribution thermalizes and the average energy decay is exponential with time. An interesting observation is that for a given nanowire size, the relaxation time does not vary much with the excitation energy.

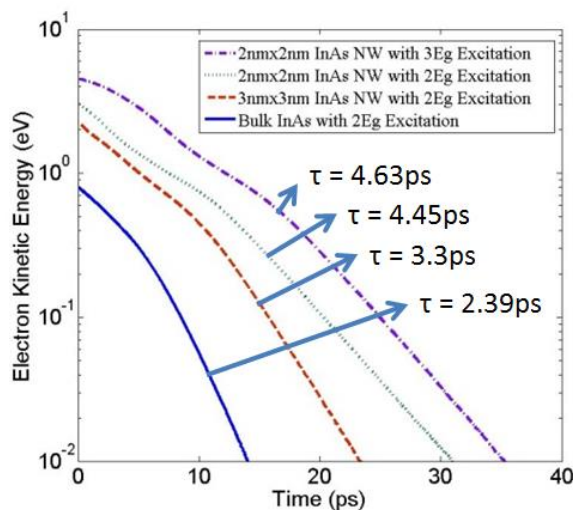


Figure 3. Energy relaxation of hot electrons in Bulk InAs, 2nmx2nm InAs NW [100] and 3nmx3nm InAs NW [100].

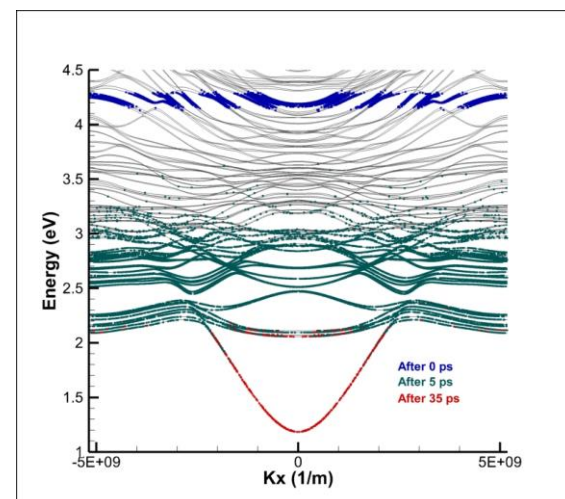


Figure 4. Carrier positions for a 2nmx2nm InAs NW [100] in k-space after photoexcitation. Each dot represents a carrier at a particular time. The initialization occurs at 0 ps.

In both cases it is noted that the relaxation time is greater for the case of nanowires when compared to the relaxation time of bulk InAs. Also smaller dimension nanowires lead to higher energy relaxation times. The initial non-exponential decay of the electrons is assumed to be due to the Gaussian nature of the initialization of carriers and the uniform distribution of carriers across the Brillouin Zone. Once

the carriers undergo sufficient scattering, the distribution both in energy and momentum reaches a physically correct distribution for excited carriers and the decay then becomes exponential as expected. The change in the distribution in carriers as it cools down can be observed in figure (4). As the carriers cool, the energy width broadens and the carriers accumulate near the band minima.

At high fields an electron “runaway” effect is also observed. At low fields the distribution is Maxwellian with a temperature of 315K, but at high fields the distribution becomes more uniform due to the runaway effect [6] as shown in figure (5). This is attributed to the nature of the 1D scattering rates which decreases in value with increase in energy within a band as seen in the inset of figure (5). This highlights the importance of full Monte Carlo simulations to simulate such devices as an assumption of the distribution function cannot be made even at moderately high electric fields.

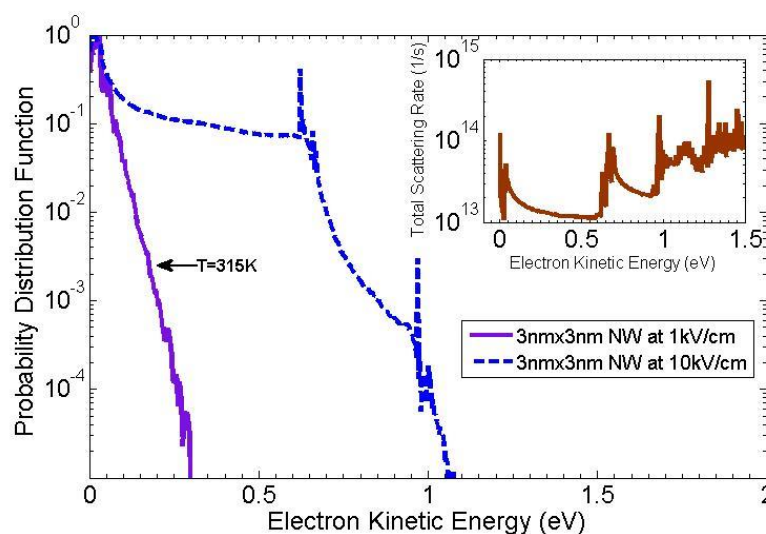


Figure 5. Distribution functions for different electric fields on a 3nm x 3nm InAs NW [100].

4. Acknowledgements

The authors would like to thank the Numerical Device Modelling group at Intel, OR for providing the funding necessary for this research and for the support of the Technische Universität München - Institute for Advanced Study, funded by the German Excellence Initiative.

References

- [1] König D, Casalenuovo K, Takeda Y, et al. 2009 *14th Intl. Conf. on Modulated Semicond. Structures*, Vol 42, Issue 10.
- [2] Kotlyar R, Linton. T D, Rios R, Giles M D, et al. 2012 *J. Appl. Phys.* **111**, 12, pp. 123718-123718-11.
- [3] Buin A K, Verma A, Anantram M P 2008, *J. Appl. Phys.* **104**, 053716.
- [4] Rössler U, *Solid State Theory – An Introduction*, 2004 Springer, New York.
- [5] Hathwar R, Saraniti M, Goodnick S M 2014, *IEEE Nano*, Pg. 645.
- [6] Dimitrev A P, Kachorovskii V Yu, Shur M S, Strosio M 2000, *Solid State Communications* **113** pp. 565-568.